Ecological Indicators 128 (2021) 107841



Contents lists available at ScienceDirect

Ecological Indicators

journal homepage: www.elsevier.com/locate/ecolind

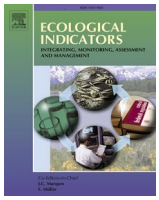



Method comparison of indirect assessments of understory leaf area index (LAI_u): A case study across the extended network of ICOS forest ecosystem sites in Europe

Jan-Peter George [a,*], Wei Yang [b], Hideki Kobayashi [c], Tobias Biermann [d], Arnaud Carrara [e], Edoardo Cremonese [f], Matthias Cuntz [g], Silvano Fares [h], Giacomo Gerosa [i], Thomas Grünwald [j], Niklas Hase [k], Michael Heliasz [d], Andreas Ibrom [l], Alexander Knohl [m], Bart Kruijt [n], Holger Lange [o], Jean-Marc Limousin [p], Denis Loustau [q], Petr Lukeš [r], Riccardo Marzuoli [s], Meelis Mölder [d], Leonardo Montagnani [t], Johan Neirynck [u], Matthias Peichl [v], Corinna Rebmann [k], Marius Schmidt [w], Francisco Ramon Lopez Serrano [x], Kamel Soudani [y], Caroline Vincke [z], Jan Pisek [a]

[a] Tartu Observatory, University of Tartu, Estonia
[b] Chiba University, Chiba, Japan
[c] JAMSTEC, Yokohama, Japan
[d] Lund University, Lund, Sweden
[e] Fundacion CEAM, Paterna, Spain
[f] ARPA Valle d'Aosta, Saint Christophe, Italy
[g] Université de Lorraine, AgroParisTech, INRAE, UMR Silva, Nancy, France
[h] CNR-National Research Council, Rome, Italy
[i] Università Cattolica del Sacro Cuore, Brescia, Italy
[j] Technische Universität Dresden, Dresden, Germany
[k] Helmholtz Centre for Environmental Research GmbH - UFZ, Leipzig, Germany
[l] Technical University of Denmark, Kongens Lyngby, Denmark
[m] University of Goettingen, Göttingen, Germany
[n] Wageningen University & Research, Wageningen, Netherlands
[o] NIBIO, Ås, Norway
[p] CEFE CNRS UMR 5175, Montpellier, France
[q] INRA, Bordeaux, France
[r] Global Change Research Institute, Academy of Sciences of the Czech Republic, Brno, Czech Republic
[s] Università Cattolica del Sacro Cuore, Brescia, Italy
[t] Free University of Bolzano, Bolzano, Italy
[u] INBO, Geraardsbergen, Belgium
[v] Department of Forest Ecology and Management, Swedish University of Agricultural Sciences, Umeå, Sweden
[w] Forschungszentrum Juelich, Juelich, Germany
[x] IER-ETSIAM, Universidad de Castilla-La Mancha, Albacete, Spain
[y] Université Paris-Saclay, CNRS, AgroParisTech, Ecologie Systématique et Evolution, 91405 Orsay, France
[z] Université Catholique de Louvain, Louvain-la-Neuve, Belgium

ARTICLE INFO

Keywords:
Forest background reflectivity
Fractional vegetation cover
Leaf area index
NDVI
Simple ratio

ABSTRACT

Leaf area index (LAI) is a key ecological indicator for describing the structure of canopies and for modelling energy exchange between atmosphere and biosphere. While LAI of the forest overstory can be accurately assessed over large spatial scales via remote sensing, LAI of the forest understory (LAI_u) is still largely ignored in ecological studies and ecosystem modelling due to the fact that it is often too complex to be destructively sampled or approximated by other site parameters. Additionally, so far only few attempts have been made to retrieve understory LAI via remote sensing, because dense canopies with high LAI are often hindering retrieval

* Corresponding author at: Tartu Observatory, University of Tartu, Observatooriumi 1, Tõravere, Estonia.
E-mail address: jan.peter.george@ut.ee (J.-P. George).

https://doi.org/10.1016/j.ecolind.2021.107841
Received 25 June 2020; Received in revised form 16 April 2021; Accepted 24 May 2021
Available online 31 May 2021
1470-160X/© 2021 The Authors. Published by Elsevier Ltd. This is an open access article under the CC BY license (http://creativecommons.org/licenses/by/4.0/).

Diversity
Understory layer

algorithms to produce meaningful estimates for understory LAI. Consequently, the forest understory still constitutes a poorly investigated research realm impeding ecological studies to properly account for its contribution to the energy absorption capacity of forest stands. This study aims to compare three conceptually different indirect retrieval methodologies for LAI_u over a diverse panel of forest understory types distributed across Europe. For this we carried out near-to-surface measurements of understory reflectance spectra as well as digital surface photography over the extended network of Integrated Carbon Observation System (ICOS) forest ecosystem sites. LAI_u was assessed by exploiting the empirical relationship between vegetation cover and light absorption (Beer-Lambert- Bouguer law) as well as by utilizing proposed relationships with two prominent vegetation indices: normalized difference vegetation index (NDVI) and simple ratio (SR). Retrievals from the three methods were significantly correlated with each other ($r = 0.63–0.99$, $RMSE = 0.53–0.72$), but exhibited also significant bias depending on the LAI scale. The NDVI based retrieval approach most likely overestimates LAI at productive sites when $LAI_u > 2$, while the simple ratio algorithm overestimates LAI_u at sites with sparse understory vegetation and presence of litter or bare soil. The purely empirical method based on the Beer-Lambert law of light absorption seems to offer a good compromise, since it provides reasonable LAI_u values at both low and higher LAI ranges. Surprisingly, LAI_u variation among sites seems to be largely decoupled from differences in climate and light permeability of the overstory, but significantly increased with vegetation diversity (expressed as species richness) and hence proposes new applications of LAI_u in ecological modelling.

1. Introduction

Leaf area index (LAI), defined as one-half the total green leaf area per unit of horizontal ground surface area (Chen and Black, 1992; Fernandes et al., 2014), is an important ecological indicator for analyzing canopy structure and constitutes a key metric for measuring interactions between the atmosphere and terrestrial ecosystems (Chen and Black, 1991; Thimonier et al., 2010). Since leaves act as a physical interface between atmosphere and biosphere, LAI strongly determines biochemical, hydrological, and atmospherical processes in canopies via rain water interception, evapotranspiration, light interception, and photosynthesis (e.g. Badhwar and MacDonald, 1986; Running and Gower, 1991; Running, 1994). While light interception in the forest canopy (i.e. overstory) is relatively well investigated and understood (e.g. Olivas et al., 2013; Schleppi et al., 2011; Thimonier et al., 2010), forest understory, which comprises all green vegetation below the canopy layer, still represents a poorly investigated research realm due to its frequently obscured character (Chen and Cihlar, 1996). Nevertheless, the contribution of the understory to the total energy absorption capacity of a forest stand can be significant and introduce potential bias of productivity estimates such as the net primary productivity (NPP) when the understory remains unaccounted for (Clark et al., 2001; Law et al., 2001). In particular, tropical woodlands and boreal forest ecosystems are well known examples for this, because the understory can even be more productive than the overstory (Clark et al., 2001; Gower et al., 2001; Black et al., 1996). The overstory and understory vegetation in forest ecosystems needs to be treated differently in carbon cycle modeling, because carbon fixed through net primary productivity has different residence times for different components (Rentch et al., 2003). Overstory and understory can possess asynchronous phenology (e.g. Ryu et al., 2014) and differences in the greening cycle of the under- and overstory species have been reported to complicate the use of simple vegetation index techniques to determine the start of growing season from Earth Observation data (Doktor et al., 2009). Consequently, satellite-derived estimates of total LAI can be strongly confounded when understory LAI information is absent (Ahl et al., 2006; Garrigues et al., 2008; Ryu et al., 2014).

A global wall-to-wall LAI dataset with separation of forest LAI for overstory and understory layers would help to improve the modeling of forest carbon and water cycles and the evaluation of forest ecosystem functions (Law and Waring 1994). Up to date, very limited efforts have been made to meet this goal. Liu et al. (2017) estimated separate overstory and understory LAI values for global needleleaf and deciduous broadleaf forests by fusing MISR and MODIS observations. Yang et al. (2015) proposed an integrating look-up table (LUT) method to remotely estimate the overstory and understory LAI for boreal forests. Kobayashi et al. (2010) proposed a satellite-based method for the overstory LAI estimation in a Siberian larch forest using the simulated relationship with the normalized difference between NIR and mid-infrared (MIR) spectral channels of Spot-Vegetation and also estimated the understory LAI as a by-product. While the efforts for understory LAI mapping with Earth Observation data have been limited, the attempts to validate the obtained retrievals have been next to non-existent.

Accurate, cost-efficient, and easy-to-implement field approaches for assessing understory leaf area index (LAI_u) are highly required in order to validate the retrievals from Earth Observation data and assist with improving productivity estimates in forest ecological studies. While a direct assessment of LAI is possible (e.g. through litter fall traps, leaf harvesting or vegetation removal), such methods have similar drawbacks to sampling overstory component, i.e. being destructive, non-repeatable, and labour-intensive. Direct approaches are also nearly impossible for some understory vegetation types such as mosses, lichens, and grasses (Weiss et al., 2004). Consequently, direct assessments are usually limited to small study areas and upscaling over different vegetation types will necessarily lead to significant bias (Jonckheere et al., 2004; Zheng and Moskal, 2009). As an alternative to direct assessment of LAI_u, a few indirect methodologies were developed that made use of either empirical or deterministic relationships between the forest background structure, light absorption patterns and reflectance properties (Campbell, 1986; Kuusk et al., 2004; Deng et al., 2006; Canisius and Chen, 2007; Yang et al., 2014). Empirical approaches make use of the fact that the amount of absorbed light in a canopy or vegetation layer is directly proportional to the concentration of absorbing elements in the layer (i.e. the Beer–Lambert–Bouguer law of light absorption). When the concentration or density as well as some key geometrical attributes of the vegetation are known, LAI_u can be approximated by exploiting this empirical relationship (e.g. Campbell, 1986; Kuusk et al., 2004; Eriksson et al., 2006; Schleppi et al., 2011). With semi-empirical and deterministic methodologies it is assumed that the forest understory has a similar composition to the mixture of shrubland, grassland, and moss (Caetano et al., 1998). LAI_u can be then retrieved using reflectances of the forest understory based on the LAI algorithms which are applicable for shrub, grass, and other non-forest biomes (Deng et al., 2006; Yang et al., 2015).

The above outlined concepts of understory LAI estimation were built upon different assumptions, vary considerably in complexity and computational requirements, and their capability of accurately assessing LAI_u depends on the spatial scale of application. However, so far no study has evaluated the comparability of these methods when applied to a common spatial scale across various understory vegetation types and when data is acquired *in-situ* (that is: via near-surface data aquisition). For this objective, we selected and produced in situ LAI_u estimates at 29 forest ecosystem sites across Europe, mainly belonging to the Integrated Carbon Observation System (ICOS) network. The rationale behind this is two-fold: first, the selected sites represent a diverse biogeographical

array of forest understory types harbouring sufficient variation for evaluating and comparing the three concepts of LAI_u assessment. Second, since one of the main objectives of the ICOS network is to provide accurate data on carbon balance (e.g. through the ICOS carbon portal (https://www.icos-cp.eu/) in forest ecosystems, our dataset can potentially inform ICOS station managers and researchers about the LAI_u range and methodological bias. Currently, the understory is often treated as unknown quantity in carbon models due to the difficulties to measure it properly *in-situ* (Luyssaert et al., 2007). Hence, the objectives of this study are: i) retrieve understory LAI estimates over the extended network of ICOS forest ecosystem sites across Europe, ii) compare retrievals among three conceptually different methodologies, ii) define levels of agreement across the measured understory LAI spectrum, and iv) discuss and evaluate potential areas of application in a broader ecological context by incorporating environmental variables such as climate, overstory properties and species diversity.

2. Materials and methods

2.1. Study area

The selected 29 study sites (Fig. 1, Table 1) comprise a large variety of forest over- and understory types and which span a latitudinal distance across Europe from 67°N (Sodankylä, Finland) to 38°N (Yeste, Spain). The investigated sites belong to five International Geosphere-Biosphere Programme (IGBP) land cover types comprising evergreen needleleaf forests (ENF, 16 sites), deciduous broadleaf forests (DBF, 7 sites), evergreen broadleaf forests (EBF, 2 sites), mixed forests (MF, 2 sites), deciduous needleleaf forests (DNF, 1 site), and open shrubland (OSH, 1 site).

2.2. Measurements of fractional cover for understory

Vertically oriented Sony Xperia Z5 Compact phone equipped with a 23 MP 1/2.3-inch multi-aspect BSI CMOS sensor, paired with an F2.0 lens was used to photograph 1 m × 1 m plots every 8 m along two 50 m long transects at each site at 3840 × 2160 pixel resolution. Fractional cover of understory vegetation was determined from the ground photos by utilizing the image analysis software *ImageJ2* (Rueden et al., 2017). Photosynthetically active plant tissue was separated from bare soil, rocks, deadwood and litter by manually adjusting hue, brightness, and saturation of digital images until all non-green background was entirely masked out. We used the *analyze*

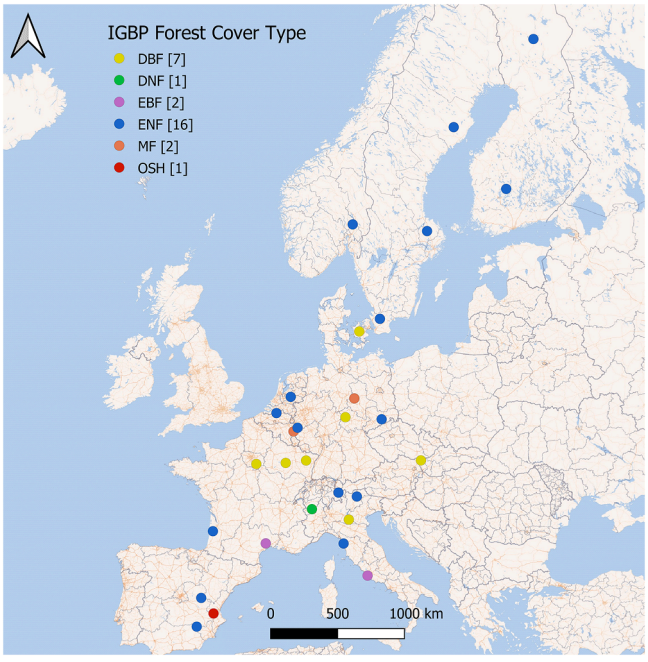

Fig. 1. Overview, geographical distribution and land cover type of the analyzed forest ecosystem research sites *particles* function in *ImageJ2* and calculated median and standard deviation of fractional vegetation cover for each of the 29 sites.

2.3. Measurements of understory spectra

In this work the reflectance factors measured by the field spectrometers are referred similarly to the satellite derived hemispherical-directional reflectance factors (HDRFs, terminology following Schaepman-Strub et al. (2006)). We approximate the field of view of the ground spectrometers to be angular, and some anisotropy was captured corresponding to normal remote sensing viewing geometry. Overview of individual in situ campaigns at each site as well as their characteristics is provided in Table 1.

Individual sites were visited between April 2017 and August 2019, mostly during the vegetation period. The understory spectra were obtained following the protocol of Rautiainen et al. (2011). The understory spectra were measured under diffuse light conditions covering the visible/near-infrared region depending on the spectrometer (see Table 1 for more details). All measurements were taken when the Sun was completely blocked by the clouds, or when direct solar radiance was totally attenuated by the long path length in tree crown layer at low solar elevations close to sunset. The understory spectra were measured every 2 m along two 50 m long transects located within the tower's footprint at each site, resulting in 25 measurement points (with three understory spectra per each measurement point) per transect. The downward-pointed spectroradiometer was held by the out-stretched hand of the operator. The area sampled during each spectral measurement was estimated to correspond approximately to a circle with a diameter of 50 cm. No fore-optics was used. Three spectra above a 10-inch 99% reflecting Spectralon SRT-99–100 white panel were recorded at the beginning and end of each transect and also along it after every four understory spectra measurement points (every 8 m).

Spectral measurements were then processed to correspond to HDRFs. Two Spectralon reflectance measurements made before and after each understory spectrum quadruplet along given transect were interpolated linearly in time to estimate the spectral irradiance for the moments when the understory spectra were recorded. A hemispherical-conical reflectance factor was obtained with an "uncalibrated" Spectralon reflectance spectrum and the interpolated irradiance.

Finally a relative spectral response function was used for Moderate Resolution Imaging Spectroradiometer (MODIS) on-board Terra to compute broadband HDRFs for red (620–670 nm) and NIR (841–876 nm) wavelengths. A simple ratio and normalized difference vegetation index (NDVI; Rouse et al., 1973) were calculated from red and near-infrared band. MODIS wavelengths were selected because its bands represent typical wavelengths that are used in vegetation remote sensing.

2.4. Models and LAI_u retrieval

2.4.1. Retrieval of LAI_u from fractional vegetation cover (LAI FC)

First, LAI_u was determined by exploiting the empirical relationship between light absorption and the fraction of ground that is covered with photosynthetically active vegetation. This relationship can be mathematically expressed as (Kuusk et al., 2004):

$$\mathbf{W} = 1 - \mathbf{exp}\left(-\frac{\mathbf{G_0 LAI_u}}{\boldsymbol{\mu_0}}\right) \quad (1)$$

with W representing the vegetation ground cover, G_0 the geometry factor describing the orientation of leaves, LAI_u is leaf area index of

Table 1
Site information and measurement device specification.

Site name	Country	Side code	IGBP land cover type	Sampling date	understory tree/shrub layer	understory herb/moss layer	Spectrometer model
Fontainebleau-Barbeau (ICOS)	FR	FR-Fon	DBF	2018/06	*Corylus spec.*		Ocean Optics FLAME-S-VIS-NIR-ES
Bilos-Salles (ICOS)	FR	FR-Bil	ENF	2018/06	*Ulex europaeus*	*Molinia coerulea, Pteridium aquilineum*	Ocean Optics FLAME-S-VIS-NIR-ES
Bosco Fontana (ICOS)	IT	IT-BFt	DBF	2018/07	*Corylus* spp., *Ruscus aculeatus*	*Hedera helix*	Ocean Optics FLAME-S-VIS-NIR-ES
Brasschaat (ICOS)	BE	BE-Bra	ENF	2019/01	*Betula spec, Quercus robur, Sorbus aucuparia*		Ocean Optics FLAME-S-VIS-NIR-ES
Castelporziano2 (ICOS)	IT	IT-Cp2	EBF	2019/01	*Phyllirea latifolia, Pistacia lentiscus*		Ocean Optics FLAME-S-VIS-NIR-ES
Cuenca de Las Majadas	ESP	ES-CMu	ENF	2018/07	*Juniperus communis, Juniperus oxycedrus, Crataegus monogyna*		Ocean Optics FLAME-S-VIS-NIR-ES
Cortes de Pallas	ESP	ES-CPa	OSH	2018/07	*Rosmarinus officinalis, Ulex parviflorus*	*Brachypodium retusum*	Ocean Optics FLAME-S-VIS-NIR-ES
Davos (ICOS)	CH	CH-Dav	ENF	2018/07		*Vaccinium* spp.	Ocean Optics FLAME-S-VIS-NIR-ES
Hainich (ICOS)	DE	DE-Hai	DBF	2018/04		*Anemone nemorosa, Allium ursinum*	Ocean Optics FLAME-S-VIS-NIR-ES
Hesse (ICOS)	FR	FR-Hes	DBF	2018/08	*Fagus sylvatica, Rubus* spp.		Ocean Optics FLAME-S-VIS-NIR-ES
Hohes Holz (ICOS)	DE	DE-HoH	MF	2018/04		*Anemone nemorosa*	Ocean Optics FLAME-S-VIS-NIR-ES
Hurdal (ICOS)	NO	NO-Hur	ENF	2018/09	*Picea abies*	*Vaccinium* spp.	Ocean Optics FLAME-S-VIS-NIR-ES
Hyltemossa (ICOS)	SE	SE-Htm	ENF	2018/09		*Sphagnum* spp.	Ocean Optics FLAME-S-VIS-NIR-ES
Hyytiälä(ICOS)	FI	FI-Hyy	ENF	2018/06	*Picea abies*	*Vaccinium* spp.	Ocean Optics FLAME-S-VIS-NIR-ES
Lanžhot (ICOS)	CZ	CZ-Lnz	DBF	2017/04		*Allium ursinum, Asarum europeum*	ASD FieldSpec 4
Loobos (ICOS)	NL	NL-Loo	ENF	2018/08	*Prunus serotina*	*Vaccinium Myrtilus, Deschampsia felexuosa*	Ocean Optics FLAME-S-VIS-NIR-ES
Montiers sur Saulx (ICOS)	FR	FR-MsS	DBF	2019/01		*Sphagnum* spp.	Ocean Optics FLAME-S-VIS-NIR-ES
Norunda (ICOS)	SE	SE-Nor	ENF	2018/10		*Vaccinium* spp.	ASD FieldSpec Pro
Puechabon (ICOS)	FR	FR-Pue	EBF	2018/06	*Buxus sempervirens*		Ocean Optics FLAME-S-VIS-NIR-ES
Renon (ICOS)	IT	IT-Ren	ENF	2018/07		*Deschampsia flexuosa, Vaccinium myrtillus, Rhododendron ferrugineum*	Ocean Optics FLAME-S-VIS-NIR-ES
San Rossore 2 (ICOS)	IT	IT-SR2	ENF	2018/07	*Ligustrum vulgare*		Ocean Optics FLAME-S-VIS-NIR-ES
Sodankylä (ICOS)	FI	FI-Sod	ENF	2017/06		*Calluna vulgaris, Vaccinium spec.*	ASD FieldSpec Pro
Soroe (ICOS)	DK	DK-Sor	DBF	2018/09	*Fagus sylvatica*	*Pteridium Aquilinum*	Ocean Optics FLAME-S-VIS-NIR-ES
Svartberget (ICOS)	SE	SE-Svb	ENF	2019/08		*Vaccinium* spp.	ASD FieldSpec Pro
Tharandt (ICOS)	DE	DE-Tha	ENF	2018/04	*Fagus sylvatica, Abies alba*	*Deschampsia flexuosa*	Ocean Optics FLAME-S-VIS-NIR-ES
Torgnon-LD	IT	IT-Tor	DNF	2018/07	*Juniperus communis*	*Rhododendron ferrugineum, Festuca varia*	Ocean Optics FLAME-S-VIS-NIR-ES
Vielsalm (ICOS)	BE	BE-Vie	MF	2018/08		*Pteridium Aquilinum*	Ocean Optics FLAME-S-VIS-NIR-ES
Wustebach (ICOS)	DE	DE-RuW	ENF	2018/08		*Deschampsia flexuosa, Deschampsia cespitosa and Molinia caerulea*	Ocean Optics FLAME-S-VIS-NIR-ES
Yeste	ESP	ES-Yst	ENF	2018/07	*Rosmarinus officinalis*	*Thymus vulgaris, Cistus clusii*	Ocean Optics FLAME-S-VIS-NIR-ES

understory, and μ_0 the cosine of the viewing angle. Assuming that G_0 for understory vegetation is 0.5 (i.e. all leaf angles are spherically distributed and foliage is randomly distributed) and that $\mu_0 = 1$ (i.e. viewing angle at nadir view is 0°) Eq. (1) can be written as:

$$LAI_u = -2ln(1 - W) \quad (2)$$

where leaf area index is solely a function of fractional vegetation cover (W) and follows the Beer-Lambert- Bouguer law of light absorption.

2.4.2. LAI_u from NDVI and radiative transfer model FLiES (LAI NDVI)

The second method for estimating LAI_u was based on the relationship between LAI and NDVI of understory vegetation derived from radiative transfer simulations (Yang et al., 2015). First, a look-up table (LUT) containing LAI and the corresponding refectance at red and near-infrared bands was generated by using the canopy radiative transfer model FLiES (Kobayashi and Iwabuchi, 2008). The vegetation structure is assumed to be homogeneous and the understory vegetation is dominated by grass and shrubs. The reflectance and transmittance of the grass category provided by Myneni et al. (1997) were used for the understory vegetation. The reflectance of the soil layer was set as the average reflectance of moss and lichen collected at a black spruce boreal forest in Alaska, USA (Kobayashi et al., 2018). Combinations of one solar zenith angle (i.e., SZA = 45°), four view zenith angle (i.e., VZA = 0°, 10°, 20°, 30°), and two view azimuth angle values (i.e., VAA = 40°, 140°) were used in the simulation. The average NDVI for each angle combination

was computed from the simulated red and near-infrared reflectances. Finally, LAI_u was estimated by searching the closest NDVI values through the previously constructed LUT with view zenith angle at nadir (VZA = 0°).

2.4.3. LAI_u retrieval from simple ratio and four-scale optical model (LAI SR)

The third method evaluated in our study was originally devised for global applications of LAI estimation (Deng et al., 2006). Briefly, the method uses land cover type-dependent relationships between LAI and vegetation indices such as the reduced simple ratio (RSR) for forests and simple ratio (SR) for grass, shrubs, and other non-forest cover types. Effective LAI is calculated based on Four Scale model simulations (Chen and Leblanc 1997) and Chebyshev polynomials with land cover type-specific algorithm coeffcients taken from look-up tables (Deng et al., 2006). The relationship between effective LAI and vegetation index is formulated as (Deng et al., 2006):

$$LE = f_{LE_VI}[f_{biome}(VI_{obs}); f_{BRDF}(\theta v, \theta s, \phi)] \quad (3)$$

where LE is the effective LAI of the understory and f_{LE_VI} a biome-specific function describing the relationship between LAI and the BRDF-modified vegetation index (VI_{obs}) at a specific view and sun angle combination ($\boldsymbol{f_{BRDF}(\theta v,\theta s,\phi)}$). f_{biome} defines the algorithm that is used (forest, shrub, grass) and f_{BRDF} quantifies the BRDF effect of the vegetation index as a function of the angular reflectance behaviour. Since the understory across all our investigated sites consisted mainly of shrubs, grasses, and other annual plants and reflectance measurements were obtained below the tree layer, we used the simple ratio (SR) and biome-specific functions designed for non-forest cover types. Non-forest cover types and their associated model coeffcients as defined in Deng et al. (2006) refer to several different vegetation classes such as open shrublands, closed shrublands and others, and we used three different cover type-dependent functions with similar characteristics (open shrubland, closed shrubland, forest savanna) for LAI_u retrieval at each site in order to better capture variation in LAI_u caused by varying model assumptions. All calculations were done in C++ with scripts provided from the study of Deng et al. (2006), which were slightly modified in order to fit our data input structure.

2.5. Method comparison and relationship between LAI_u and environmental variables

The three LAI retrievals were compared among the 29 sites by pairwise calculation of Pearson-moment-correlation, coeffcient of determination (R^2), and root-mean-square error (RMSE). Furthermore, since we were particularly interested to know whether the LAI ranges within the three methods give comparable estimates, we calculated pairwise limits of agreement (Altman and Bland, 1983). Limits of agreement (LoA) have been widely used in evidence-based medicine in order to quantify the bias between two or more clinical test settings. Since our three methods differ greatly in model complexity, computational demand, and physical assumptions, non-significant deviations among the three methods across the investigated LAI range would speak in favour of the method that makes least model assumptions and is also easiest to implement. We pairwisely regressed the difference between methods against the mean (the so-called Bland-Altman-plot). The pairwise relative bias among methods was calculated as the mean of all differences across the 29 sites. The agreement interval in which 95% of the differences fall was calculated as ±1.96 × SD with SD being the standard deviation of the pairwise differences.

Finally, we explored the relationship between LAI_u retrievals and environmental variables at the 29 sites. Strong correlations between retrieved LAI_u estimates and variables that are nowadays relatively easy to obtain from databases (e.g. latitude, longitude, and climate parameters) may suggest that an approximation of understory LAI is possible without the need for time-consuming data gathering and computation. For example, Iio et al. (2014) revealed significant relationships between field-observed LAI and temperature/precipitation across plant functional types. On a global basis their results suggest that LAI is mainly limited by temperature and water availability, in particular under cool and dry climate conditions. In order to test this hypothesis for LAI_u, we obtained 80 long-term climatic variables with 1 km^2 spatial resolution for the ICOS sites from the ECLIPS 2.0 dataset (Chakraborty et al., 2020). Briefly, the ECLIPS dataset contains gridded annual, seasonal, and monthly climate variables for past periods (1960–2010) and wasvalidated with observations from a >4000 weather stations (Klok and Klein Tank, 2009). A detailed description of the 80 climatic variables can be found in the Supplementary Material S1. In order to reduce the complexity of this dataset, LAI_u was regressed against the first two principal components of this climatic site information. Additionally, we used overstory LAI (LAI_o) and understory species richness as a predictors of LAI_u. Information on overstory LAI for the analyzed ICOS sites was obtained for 25 of the analyzed sites from already published literature (Supplementary Material S2) and was aggregated to mean values in cases where several measurements per site were made or reported. Since overstory LAI was assessed by using different methods and at different dates compared to LAI_u, we are using this information only as a broad surrogate for understory light availability and for this purpose only. Species richness is simply defined as the total number of species which are represented in a biological community and was assessed by visually inspecting the ground photos. We used the *prcomp* function in R (R Core Team, 2017) for the principal component analysis of climate data and performed linear models between LAI_u retrievals and the four environmental predictors (two climate PCs, LAI_o, and species richness) with the *lm* function in the R computational environment.

3. Results

3.1. Understory LAI variation among study sites and land cover types

Overall the retrieved understory LAI estimates varied strongly among the investigated sites at the given point in a season when in situ measurements were taken. The majority of sites had low to moderate LAI_u values in the range between 0 and 1 (18 sites), 9 sites had LAI_u values between 1 and 2, and 2 sites showed relatively higher LAI_u values >2 (Table 2). LAI_u was higher in evergreen and decidous needleleaf forests, and in decidous broadleaf forests (0.96, 2.48, 1.05, respectively) compared to evergreen broadleaf forests, mixed forests, and open shrubland (0.53, 0.41, 0.89, respectively; note that DNF and OSH are each represented by only one site) (Fig. 2).

3.2. Correlation among retrieval methods

Since we obtained one LAI estimate per site for the fractional cover method and the NDVI method, LAI values that were derived for the three cover types with similar characteristics from the simple ratio method were averaged for subsequent analyses. However, the standard deviation of LAI_u among the three chosen cover types was low for all sites and was on average 0.05 m^2/m^2 (Fig. 3).

The three applied methods showed moderate to high correlation when compared pairwisely. LAI derived from fractional vegetation cover was moderately correlated with both methods that used vegetation indices (correlation coefficients 0.63 and 0.68, respectively). In contrast, LAI derived from NDVI and LAI obtained from SR showed very strong correlation and the lowest root mean square error among the three comparisons (r = 0.99, RMSE = 0.53) (Fig. 4a-c).

3.3. Limits of agreement (LoA) and pairwise bias among methods

Mean bias among methods ranged from 0.016 (fractional cover vs. NDVI) to −0.34 (NDVI vs. SR) with errors of pair-wise differences

Table 2
LAI_u retrievals per site and mean LAI_u across the three methods. LAI_{FC} = Fractional cover method, LAI_{NDVI} = NDVI-based retrieval, LAI_{SR} = Simple-ratio based method.

Site	LAI_{FC}	LAI_{NDVI}	LAI_{SR}	mean LAI_u
FR-Fon	0.96	0.71	1.23	0.97
FR-Bil	2.48	1.48	1.58	1.85
IT-BFt	1.75	3.28	2.46	2.50
BE-Bra	0.12	0.16	0.73	0.34
IT-Cp2	0.06	0.20	0.80	0.36
ES-CMu	0.02	0.17	0.79	0.32
ES-CPa	1.11	0.45	1.10	0.89
CH-Dav	1.79	0.34	0.89	1.01
DE-Hai	0.43	0.58	1.07	0.69
FR-Hes	0.01	0.06	0.55	0.21
DE-HoH	0.29	0.23	0.83	0.45
NO-Hur	1.67	1.59	1.55	1.61
SE-Htm	1.04	1.18	1.45	1.22
FI-Hyy	1.67	1.32	1.49	1.50
CZ-Lnz	1.34	1.92	1.78	1.68
NL-Loo	0.43	0.13	0.74	0.43
FR-MsS	0.05	0.55	1.07	0.56
SE-Nor	1.45	1.04	1.34	1.27
FR-Pue	0.87	0.37	0.89	0.71
IT-Ren	1.36	0.93	1.40	1.23
IT-SR2	0.14	0.23	0.96	0.44
FI-Sod	0.99	0.24	0.81	0.68
DK-Sor	0.28	0.47	0.97	0.57
SE-Svb	1.40	1.96	1.73	1.70
DE-Tha	0.55	0.54	1.01	0.70
IT-Tor	1.24	3.60	2.58	2.48
BE-Vie	0.19	0.17	0.74	0.37
DE-RuW	0.92	0.38	1.00	0.77
ES-Yst	0.22	0.05	0.60	0.29

between 0.07 and 0.50 (Table 3). Systematic bias among the three retrievals appeared at high LAI_u ranges (LAI_u of 2–3) where the NDVI method gave significantly higher LAI_u estimates than the other two methods (Fig. 4d-f, black points outside the blue dashed lines). LAI_u derived from simple ratio gave two significantly lower estimates when compared to the fractional cover method at medium ($LAI_u \sim 1.3$) and at high ranges ($LAI_u \sim 2.0$), but the deviations were of rather random character.

3.4. Relationship between understory LAI and environmental site parameters

The first two principal components of the 83 long-term climatic variables explained 73.4% and 13.7%, respectively. PC1 was mainly associated with temperature variables while PC2 included mainly variables associated with precipitation regime at the investigated sites. However, the relationships between both PCs and LAI_u were not significant ($p > 0.05$ in both linear models, Supplementary Material S1).

Species richness varied significantly among the 29 sites and ranged from 2 counted species (Hyltemossa) to 15 understory species (Lanžhot). Highest LAI_u was found at sites with intermediate overstory leaf area index ($LAI_o \sim 4\ m^2/m^2$), but there was otherwise no significant relationship among indices (Fig. 5a). In contrast, the number of species that were counted within sites had a significant positive effect on understory LAI when calculated as average across the three methods (slope: 0.07, $R^2 = 0.14$, $p < 0.001$, Fig. 5b) as well as for each method separately (data not shown).

4. Discussion

Assessing biophysical properties of the forest understory is an important field of research in order to inform forest ecological research and modeling of forest ecosystem productivity. The understory layer still constitutes a cryptic quantity in many ecological studies due to the fact that it is often too complex to be directly assessed at larger spatial scales (Luyssaert et al., 2007; Clark et al., 2001). Neverthless, our data gives evidence that the contribution of understory to the entire energy absorption capacity of a forest stand can be significant, since we found LAI_u values that were partly in the range of forest overstories, especially in boreal forests and temperate woodlands (e.g. Black et al., 1996; Gower et al., 1999). Satellite-based assessments of understory LAI would be preferable, because they could provide information at regional and global scales in relatively short time. However, its usability is often limited to rather sparse and open canopies, because dense and closed canopies will retain the reflection signal of the forest background (Pisek

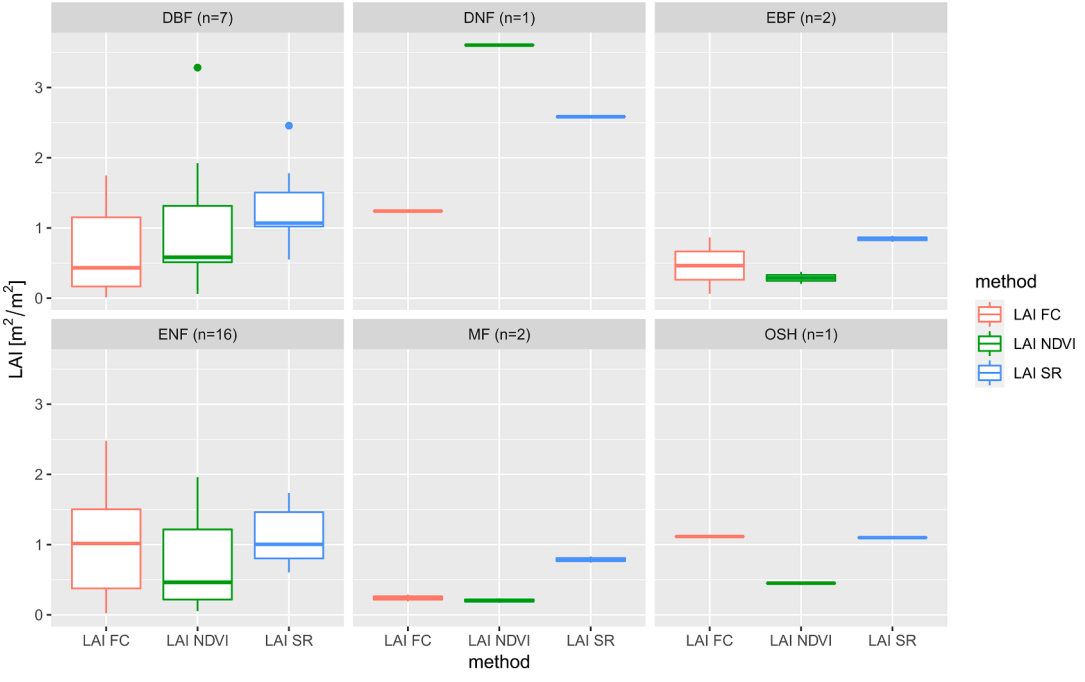

Fig. 2. Understory LAI distribution for each retrieval method and investigated forest cover type.

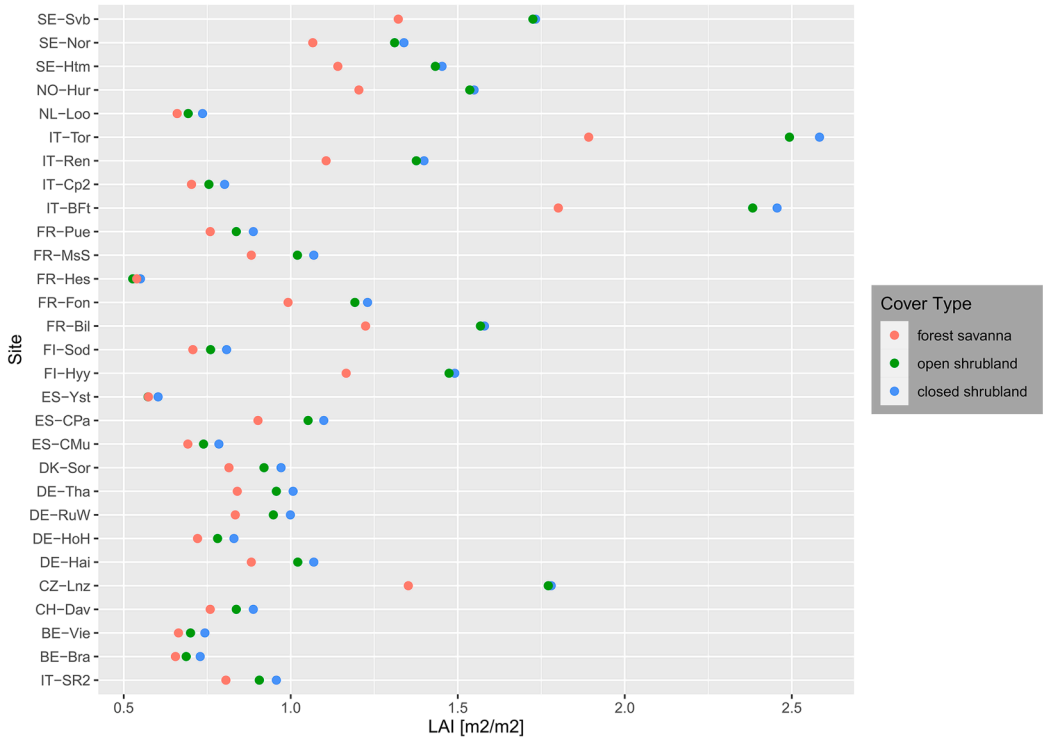

Fig. 3. Understory LAI variation among the three different land cover types as defined in Deng et al. (2006) for the LAI_{SR} method.

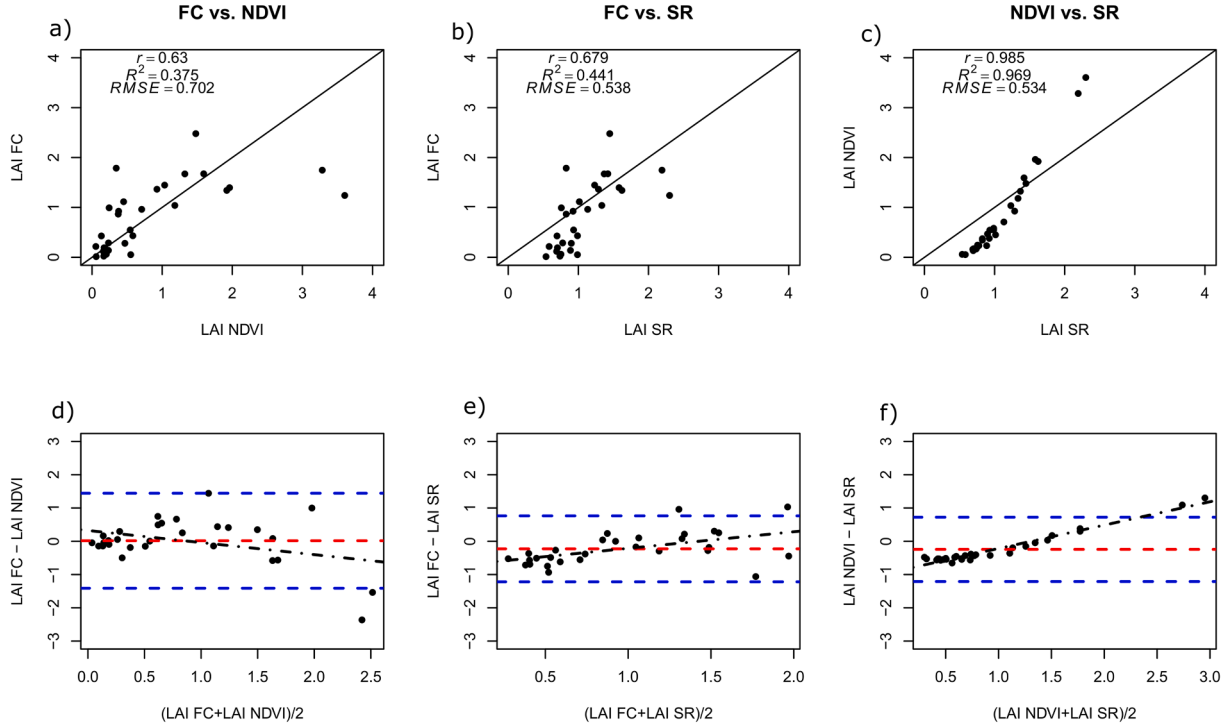

Fig. 4. Pairwise correlation of the three evaluated retrieval methodologies (a-c) and their respective biases expressed as Bland-Altman-diagrams (d-f). The red dashed line in plots d-f shows the mean bias and the blue dashed lines show proportional biases expressed as 95% confidence intervals of error distribution. The blue lines can be interpreted as upper/lower limits of agreement. Black dashed lines show the linear regression of bias against mean of the two methods per site. (For interpretation of the references to color in this figure legend, the reader is referred to the web version of this article.

et al., 2016). Since LAI algorithms using satellite products are usually landcover type-dependent, missclassifications of the forest type in the underlying land cover map can induce errors to the retrieved LAI product (Jiao et al., 2014). Hence, we carried out an assessment approach based on *in-situ* measurements below the overstory by comparing three conceptually different retrieval methodologies for leaf area index of the understory layer.

Table 3
Pairwise mean bias and standard deviation (in parentheses) among the three methods.

	LAI_{FC}	LAI_{NDVI}	LAI_{SR}
LAI_{FC}	–		
LAI_{NDVI}	0.016 (0.74)	–	
LAI_{SR}	−0.320 (0.501)	−0.336 (0.425)	–

4.1. Magnitude and variation of understory LAI across forest ecosystem ICOS and fluxnet sites

Our study area encompassed boreal, temperate as well as mediterranean ecosystems with diverse forest ecosystem understory types. Highest LAI_u values were found in a decidous needleleaf forest (Torgnon: 1.2–3.6 m^2/m^2) as well as in decidous broadleaf forest (Bosco Fontana: 1.7–3.3 m^2/m^2). Both sites are characterized by an intermediate and light permeable overstory (oak and hornbeam in Bosco Fontana; European larch in Torgnon) with a densely developed shrub layer (*Ruscus, Corylus* in Bosco Fontana; *Juniperus* and *Vaccinium* in Torgnon) in the understory. In particular, *Ruscus aculeatus* is known to be an extremely shade- and drought-tolerant understory species having green and photosynthetically active stems (Pivovaroff et al., 2014). Since the species occurred along the transect at the Bosco Fontana site at high frequency, we presume that this strongly contributed to the high LAI_u value retrieval. The fractional vegetation cover in Torgnon was very similar to those previously reported from other larch forests. Kushida et al. (2007) assessed the influence of understory vegetation in a Siberian larch forest and found a very high contribution of the understory vegetation to total leaf area because of the relatively high proportion of light transmitted through the sparse overstory canopy. The median fractional cover in Torgnon was very similar as compared to the study with Siberian larch (46% in Torgnon vs. 52% in Kushida et al. (2007)) and this probably explains the high LAI_u found in our study. It should be however noted that deciduous needleleaf and evergreen broadleaf forests were only poorly represented in our dataset (n = 1 for DNF and n = 3 for EBF), which makes it difficult to generalize our findings.

Intermediate LAI_u retrievals were found in evergreen needleleaf forests situated at high latitudes (Hurdal, Hyltemossa, Hyytiälä, Norunda, Svartberget) and were in the range between 0.7 and 1.6. This finding corroborates earlier studies which found the strongest influence of the understory vegetation in forest ecosystems situated at high latitudes (e.g. Liu et al., 2017; Jiao et al., 2014). The values that were retrieved in this study are close to those that were obtained by inversion of a two-layer canopy reflectance model that was applied over a diverse panel of understory types in boreal forest ecosystems (Kuusk et al., 2004). For example, Kuusk et al. (2004) reported effective LAI values in *Vaccinium*-dominated Scots pine and Norway spruce forests in the range between 0.4–2.3 m^2/m^2. These understory types come closest to those analyzed in our study, since *Vaccinium spec.* was the dominating understory species in all mentioned sites above except Hyltemossa.

4.2. Differences among retrieval methodologies and limits of agreement

Substantial differences among retrieval methodologies will necessarily bias LAI estimates, because the obtained values will change depending on the applied method. Some methodologies may capture LAI better at low or intermediate LAI ranges, while others provide more realistic estimates at higher LAI ranges. We analyzed the uncertainty, pairwise bias and limits of agreement (LoA) among the three methodologies. We found differences (expressed as RMSE) in the range of 0.53–0.7 LAI units, which is slightly lower compared to uncertainties among retrieval methodologies of total LAI. These were found to be between 0.56 and 1.25 LAI units when the most common retrieval methods ECOCLIMAP, CYCLOPES, GLOBCARBON, and MODIS were compared (Garrigues et al., 2008). However, an important aspect is whether the bias among methods is of random or systematic nature, because only the latter would allow to recommend one method instead of the other. LAI_u derived from NDVI gave significantly higher estimates compared to the other two methods at higher LAI ranges ($LAI_u > 2$) (Fig. 4d,f). This resulted in unrealistically high retrievals for the Bosco Fontana and Torgnon site with this method, which were twice as high compared to the fractional cover method. Technically, the dependency of the retrieved LAI from the main parameter has a different strength among the three methods: while LAI_{FC} and LAI_{SR} show a relatively moderate LAI increase towards higher vegetation cover or SR values, LAI_{NDVI} exhibits a strong exponential relationship between LAI and observed NDVI (Fig. 6). Consequently, the method most likely overestimates LAI_u at very productive sites with dense understory and NDVI > 0.7.

In contrast, LAI_{SR} showed higher values most notably at low LAI

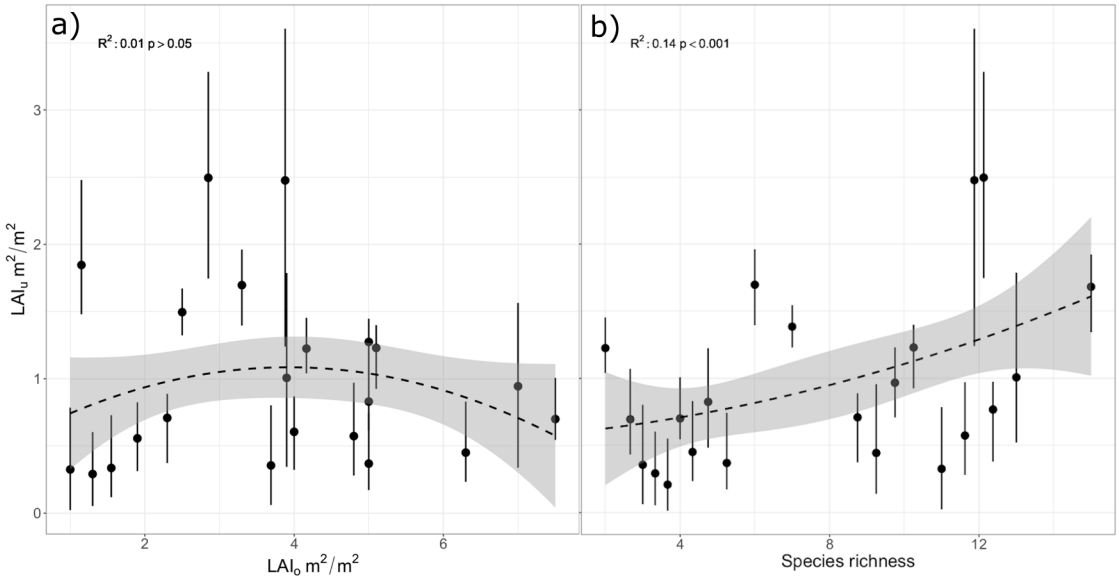

Fig. 5. Relationship between retrieved LAI_u and environmental parameters: a) overstory LAI for the 29 sites from published literature and b) species richness obtained from ground photos. Errorbars display variation among the three LAI_u retrieval methods. Note that overstory LAI values were not available for four sites (Cortes de Pallas, Hurdal, and Montiers).

ranges compared to the other two methods, although the bias was inside the credibility intervals in both cases. LAI values below 0.5 were not retrieved at all by LAI_{SR}, which questions its suitability in areas with very sparse ground vegetation such as temperate forests with dense overstory and dry mediterranean shrublands with low site productivity. Sites with low LAI_u appeared in our dataset mainly at low latitudes (Yeste, San Rossore, Cuenca de las Majadas, Castelporziano) as well as in broadleaf forest ecosystems with dense overstory vegetation (e.g. Hohes Holz, Vielsalm). The simple ratio is indeed known to be vulnerable against occurrence of litter and bare soil which often leads to considerably higher LAI values when compared to other vegetation indices (e.g. Zhu et al., 2010). As such, very high NIR reflectances were observed at the Hohes Holz and Cuenca de las Majadas (CdM) sites and both were characterized by high amount of exposed leaf litter and dessicated grass remnants, respectively.

The purely empirical method (LAI_{FC}) which is based on a simple physical law seems to capture the whole spectrum of LAI_u well without significant bias at either high or low ends. However, for the ease of simplicity and for reasons of comparability we assumed that all understory vegetation has spherical leaf angles and random distribution. While species-specific information on leaf inclination angles exists nowadays for many trees and shrubs (e.g. Chianucci et al., 2018), future development of such databases for other forest perennials and annual plants could further improve LAI_u estimation when the fractional vegetation cover method is used.

4.3. LAI variation among selected land cover types for simple ratio

For comparison we used direct retrievals obtained from vegetation cover and NDVI, since both are land cover-independent. However, the method by Deng et al. (2006), which is based on the simple ratio, was designed in a way that model coeffcients are selected depending on the respective land cover type. We ran the model with three different land cover types which refer to different shrub biomes and used the average across the three types for comparison. Nevertheless, the variation among the three selected cover types was small in all cases and did on average not exceed 0.05 LAI units. Consequently, choosing one shrub biome instead of the other for LAI_u calculations will most likely not lead to a significant bias of LAI_u retrieval. This corroborates earlier studies which investigated the effect of different land-cover type assumptions on global LAI retrieval and which found only little differences among them as well (Liu et al., 2017).

4.4. Relationship between understory leaf area index and environmental parameters

Since productivity of forest ecosystems in general is largely driven by climatic conditions such as winter temperatures or drought regime (Schuur, 2003), we wanted to test whether biogeographical variation in leaf area index of the understory (as a surrogate of site understory productivity) shows similar strong relationships with such drivers. However, differences in LAI_u were poorly correlated with long-term site climatic conditions. Iio et al. (2014) demonstrated that field-based LAI shows strong relationship with temperature and water availability when analysed at global scale, but pointed out that such relationships can strongly differ among plant functional types. In addition, Wright et al. (2004) found that most of the global variation in leaf traits occurs among co-existing species within sites rather than among different climates across sites. In the light of these studies we conclude that the non-significant relationship between LAI_u and key climatic parameters can be best explained by the diverse panel of understory plant functional types and plant ecological communities that were analyzed. Additionally, variation in LAI_u showed no causal relationship with increasing or decreasing leaf area index of the overstory, although such relationships were found in earlier studies at smaller spatial scale (e.g. Chianucci et al., 2014; Eriksson et al., 2006). Nevertheless, our findings suggest that biogeographical differences in LAI_u are not soley driven by light availability, but also by other factors such as soil properties, fire occurrence, and other abiotic stress regimes (e.g. Gentry and Emmons, 1987).

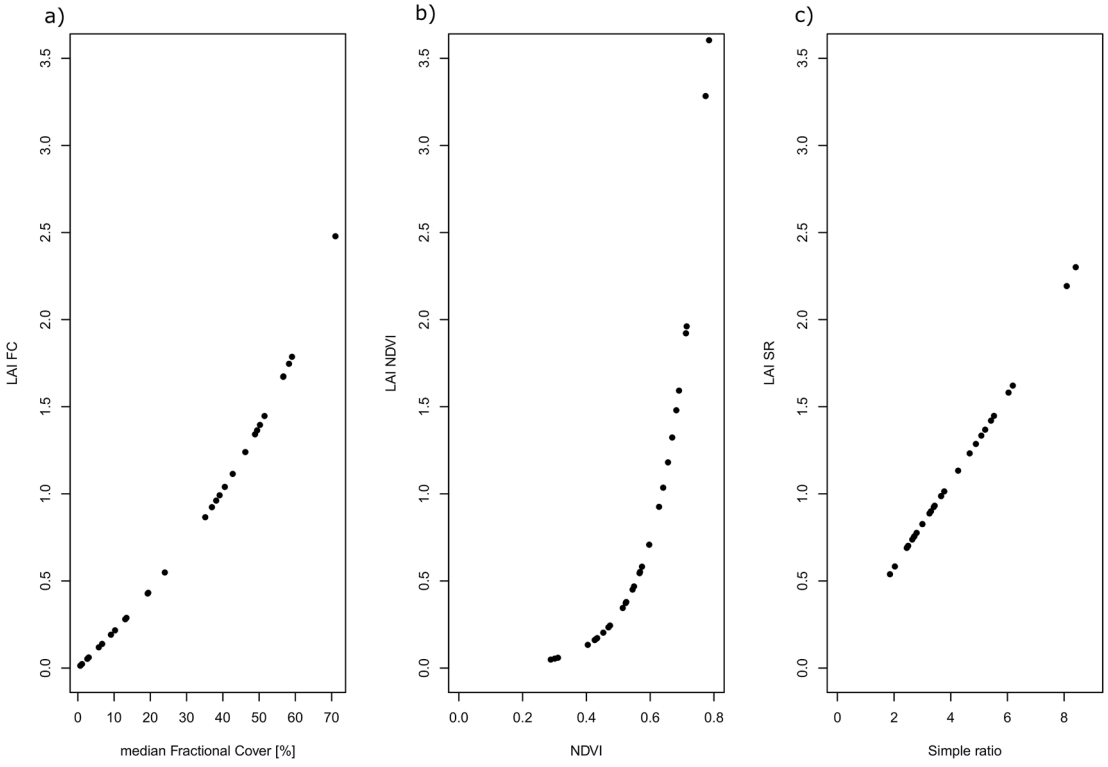

Fig. 6. Retrieved understory LAI in relation to its main parameter - fractional cover [%], NDVI, and SR, respectively. Black dots represent the mean LAI_u of the investigated sites.

In contrast to climate and overstory properties, species richness had a significant effect on LAI_u variation so that sites that are harbouring more species show greater understory LAI (Fig. 5b). The relationship was significant over all three retrieval methodologies, but was most strongly pronounced for LAI_{NDVI} which showed a steep slope towards higher species richness values. Such relationships between vegetation indices and vegetation diversity parameters were found in other studies as well (e.g. Gould, 2000; Oindo and Skidmore, 2002) and discussed as a potential remote sensing tool in order to predict plant diversity from vegetation indices at larger spatial scales (Rocchini et al., 2004). In turn, we hypothesized that LAI of the forest understory may be inversely predicted when key vegetation parameters are known, for instance from detailed survey data available for most of the investigated sites. Our assessment represents a first step that may be more thoroughly investigated and probably substantiated with more data and additional parameters in the future. Such approximations could indeed assist energy exchange modelling in forest ecosystems by approximating the largely unkown quantity that the understory LAI still constitutes in most of the studies.

5. Conclusions

In this study we compared three conceptually different retrieval methodologies for understory LAI across a wide panel of 29 different understory types. We found significant heterogeneity of LAI_u in space that can be attributed to differences in vegetation diversity, but not to variation in biogeography and climate among sites or differences in overstory properties. Retrievals obtained from the three methods were significantly correlated with each other, but performed differently at specific LAI ranges. In order to derive meaningful and reliable in situ LAI_u estimates, we recommend the given method might be selected depending on the overall conditions of the respective site. LAI_u derived from fractional vegetation cover (previously applied by e.g. Heiskanen et al. (2012)) seems to be a good compromise for indirect in situ LAI_u estimation given that it was capable of retrieving LAI_u at both low and high LAI ranges without constraints of reflectivity issues related to presence of bare soil or dense vegetation and saturation. Furthermore, this method makes least model assumptions and is easy-to-implement by using standard equipment such as a digital camera and open-source image analysis software. Our results are pertinent to future efforts to provide more field data for further evaluation and comparison of regional and global understory LAI products such as GLOBMAP (Liu et al., 2017) and others.

CRediT authorship contribution statement

Jan-Peter George: Formal analysis, Methodology, Writing - original draft, Visualization. **Wei Yang:** Software, Resources, Writing - review & editing. **Hideki Kobayashi:** Software, Resources, Writing - review & editing. **Tobias Biermann:** Resources, Writing - review & editing. **Arnaud Carrara:** Resources, Writing - review & editing. **Edoardo Cremonese:** Resources, Writing - review & editing. **Matthias Cuntz:** Resources, Writing - review & editing. **Silvano Fares:** Resources, Writing - review & editing. **Giacomo Gerosa:** Resources, Writing - review & editing. **Thomas Grünwald:** Resources, Writing - review & editing. **Niklas Hase:** Resources, Writing - review & editing. **Michael Heliasz:** Resources, Writing - review & editing. **Andreas Ibrom:** Resources, Writing - review & editing. **Alexander Knohl:** Resources, Writing - review & editing. **Bart Kruijt:** Resources, Writing - review & editing. **Holger Lange:** Resources, Writing - review & editing. **Jean-Marc Limousin:** Resources, Writing - review & editing. **Denis Loustau:** Resources, Writing - review & editing. **Petr Lukeš:** Resources, Writing - review & editing. **Riccardo Marzuoli:** Resources, Writing - review & editing. **Meelis Mölder:** Resources, Writing - review & editing. **Leonardo Montagnani:** Resources, Writing - review & editing. **Johan Neirynck:** Resources, Writing - review & editing. **Matthias Peichl:** Resources, Writing - review & editing. **Corinna Rebmann:** Resources, Writing - review & editing. **Marius Schmidt:** Resources, Writing - review & editing. **Francisco Ramon Lopez Serrano:** Resources, Writing - review & editing. **Kamel Soudani:** Resources, Writing - review & editing. **Caroline Vincke:** Resources, Writing - review & editing. **Jan Pisek:** Conceptualization, Methodology, Writing - original draft, Supervision, Project administration, Funding acquisition.

Declaration of Competing Interest

The authors declare that they have no known competing financial interests or personal relationships that could have appeared to influence the work reported in this paper.

Acknowledgements

This study was supported from Estonian Research Council Grant PUT1355 and Mobilitas Pluss MOBERC11. Field campaign at Brasschaat site was funded by the Transnational Access scheme of eLTER (Horizon 2020 project grant agreement no. 654359).

Appendix A. Supplementary data

Supplementary data to this article can be found online at https://doi.org/10.1016/j.ecolind.2021.107841.

References

Ahl, D.E., Gower, S.T., Burrows, S.N., Shabanov, N.V., Myneni, R.B., Knyazikhin, Y., 2006. Monitoring spring canopy phenology of a deciduous broadleaf forest using MODIS. Remote Sens. Environ. 104 (1), 88–95.
Altman, D.G., Bland, J.M., 1983. Measurement in medicine: the analysis of method comparison studies. *J. Roy. Stat. Soc.*: Series D (The Statistician) 32 (3), 307–317.
Badhwar, G.D., MacDonald, R.B., 1986. Satellite-derived leaf-area-index and vegetation maps as input to global carbon cycle models-a hierarchical approach. Int. J. Remote Sens. 7 (2), 265–281.
Black, T.A., Den Hartog, G., Neumann, H.H., Blanken, P.D., Yang, P.C., Russell, C., Novak, M.D., 1996. Annual cycles of water vapour and carbon dioxide fluxes in and above a boreal aspen forest. Glob. Change Biol. 2 (3), 219–229.
Caetano, M.R., Huete, A.R., Pereira, J.M.C., Ni, W., 1998. December). Forest understory characterization at regional levels with satellite data: A conceptual approach. In: Remote Sensing for Agriculture, Ecosystems, and Hydrology, Vol. 3499. International Society for Optics and Photonics, pp. 245–256.
Campbell, G.S., 1986. Extinction coefficients for radiation in plant canopies calculated using an ellipsoidal inclination angle distribution. Agric. For. Meteorol. 36 (4), 317–321.
Canisius, F., Chen, J.M., 2007. Retrieving forest background reflectance in a boreal region from Multi-angle Imaging SpectroRadiometer (MISR) data. Remote Sens. Environ. 107 (1-2), 312–321.
Chakraborty, D., Dobor, L., Zolles, A., Hlásny, T., Schueler, S., 2020. High-resolution gridded climate data for Europe based on bias-corrected EURO-CORDEX: The ECLIPS dataset. Geosci. Data J.
Chen, J.M., Cihlar, J., 1996. Retrieving leaf area index of boreal conifer forests using Landsat TM images. Remote Sens. Environ. 55 (2), 153–162.
Chen, J.M., Black, T.A., 1992. Defining leaf area index for non-flat leaves. Plant Cell Environ. 15 (4), 421–429.
Chen, J.M., Black, T.A., 1991. Measuring leaf area index of plant canopies with branch architecture. Agric. For. Meteorol. 57 (1-3), 1–12.
Chianucci, F., Pisek, J., Raabe, K., Marchino, L., Ferrara, C., Corona, P., 2018. A dataset of leaf inclination angles for temperate and boreal broadleaf woody species. Ann. For. Sci. 75 (2), 50.
Chianucci, F., Puletti, N., Venturi, E., Cutini, A., Chiavetta, U., 2014. Photographic assessment of overstory and understory leaf area index in beech forests under different management regimes in Central Italy. For. Stud. 61 (1), 27–34.
Clark, D.A., Brown, S., Kicklighter, D.W., Chambers, J.Q., Thomlinson, J.R., Ni, J., 2001. Measuring net primary production in forests: concepts and field methods. Ecol. Appl. 11 (2), 356–370.
Deng, F., Chen, J.M., Plummer, S., Chen, M., Pisek, J., 2006. Algorithm for global leaf area index retrieval using satellite imagery. IEEE Trans. Geosci. Remote Sens. 44 (8), 2219–2229.
Doktor, D., Bondeau, A., Koslowski, D., Badeck, F.-W., 2009. Influence of heterogeneous landscapes on computed green-up dates based on daily AVHRR NDVI observations. Remote Sens. Environ. 113 (12), 2618–2632.
Eriksson, H.M., Eklundh, L., Kuusk, A., Nilson, T., 2006. Impact of understory vegetation on forest canopy reflectance and remotely sensed LAI estimates. Remote Sens. Environ. 103 (4), 408–418.

Fernandes, R., Plummer, S., Nightingale, J., Baret, F., Camacho, F., Fang, H., Garrigues, S., Gobron, N., Lang, M., Lacaze, R., et al. (2014). Global Leaf Area Index Product Validation Good Practices. Version 2.0. In Best Practice for Satellite-Derived Land Product Validation: Land Product Validation Subgroup (WGCV/CEOS); Schaepman-Strub, G., Román, M., Nickeson, J., Eds.; NASA: Greenbelt, MD, USA, p. 76.

Garrigues, S., Lacaze, R., Baret, F.J.T.M., Morisette, J.T., Weiss, M., Nickeson, J.E., Knyazikhin, Y., 2008. Validation and intercomparison of global Leaf Area Index products derived from remote sensing data. J. Geophys. Res. Biogeosci. 113 (G2).

Gentry, A.H., Emmons, L.H., 1987. Geographical variation in fertility, phenology, and composition of the understory of Neotropical forests. Biotropica 19 (3), 216. https://doi.org/10.2307/2388339.

Gould, W., 2000. Remote sensing of vegetation, plant species richness, and regional biodiversity hotspots. Ecol. Appl. 10 (6), 1861–1870.

Gower, S.T., Krankina, O., Olson, R.J., Apps, M., Linder, S., Wang, C., 2001. Net primary production and carbon allocation patterns of boreal forest ecosystems. Ecol. Appl. 11 (5), 1395–1411.

Gower, S.T., Kucharik, C.J., Norman, J.M., 1999. Direct and indirect estimation of leaf area index, fAPAR, and net primary production of terrestrial ecosystems. Remote Sens. Environ. 70 (1), 29–51.

Heiskanen, J., Rautiainen, M., Stenberg, P., Mõttus, M., Vesanto, V.-H., Korhonen, L., Majasalmi, T., 2012. Seasonal variation in MODIS LAI for a boreal forest area in Finland. Remote Sens. Environ. 126, 104–115.

Iio, A., Hikosaka, K., Anten, N.P.R., Nakagawa, Y., Ito, A., 2014. Global dependence of field-observed leaf area index in woody species on climate: a systematic review. Glob. Ecol. Biogeogr. 23 (3), 274–285.

Jiao, T., Liu, R., Liu, Y., Pisek, J., Chen, J.M., 2014. Mapping global seasonal forest background reflectivity with Multi-angle Imaging Spectroradiometer data. J. Geophys. Res. Biogeosci. 119 (6), 1063–1077.

Jonckheere, I., Fleck, S., Nackaerts, K., Muys, B., Coppin, P., Weiss, M., Baret, F., 2004. Review of methods for in situ leaf area index determination: Part I. Theories, sensors and hemispherical photography. Agric. For. Meteorol. 121 (1-2), 19–35.

Klok, E.J., Klein Tank, A.M.G., 2009. Updated and extended European dataset of daily climate observations. Int. J. Climatol. 29 (8), 1182–1191.

Kobayashi, H., Suzuki, R., Yang, W., Ikawa, H., Inoue, T., Nagano, H., Kim, Y., 2018. Spectral reflectance and associated photograph of boreal forest understory formation in interior Alaska. Polar Data J. 2, 14–29.

Kobayashi, H., Delbart, N., Suzuki, R., Kushida, K., 2010. A satellite-based method for monitoring seasonality in the overstory leaf area index of Siberian larch forest. J. Geophys. Res. Biogeosci. 115 (G1).

KOBAYASHI, H., IWABUCHI, H., 2008. A coupled 1-D atmosphere and 3-D canopy radiative transfer model for canopy reflectance, light environment, and photosynthesis simulation in a heterogeneous landscape. Remote Sens. Environ. 112 (1), 173–185.

Kushida, K., Isaev, A.P., Maximov, T.C., Takao, G., Fukuda, M., 2007. Remote sensing of upper canopy leaf area index and forest floor vegetation cover as indicators of net primary productivity in a Siberian larch forest. J. Geophys. Res. Biogeosci. 112 (G2).

Kuusk, A., Lang, M., Nilson, T., 2004. Simulation of the reflectance of ground vegetation in sub-boreal forests. Agric. For. Meteorol. 126 (1-2), 33–46.

Law, B.E., Van Tuyl, S., Cescatti, A., Baldocchi, D.D., 2001. Estimation of leaf area index in open-canopy ponderosa pine forests at different successional stages and management regimes in Oregon. Agric. For. Meteorol. 108 (1), 1–14.

Law, B.E., Waring, R.H., 1994. Remote sensing of leaf area index and radiation intercepted by understory vegetation. Ecol. Appl. 4 (2), 272–279.

Liu, Y., Liu, R., Pisek, J., Chen, J.M., 2017. Separating overstory and understory leaf area indices for global needleleaf and deciduous broadleaf forests by fusion of MODIS and MISR data. Biogeosciences 14 (5), 1093–1110.

Luyssaert, S., Inglima, I., Jung, M., Richardson, A.D., Reichstein, M., Papale, D., Aragao, L.E.O.C., 2007. CO2 balance of boreal, temperate, and tropical forests derived from a global database. Glob. Change Biol. 13 (12), 2509–2537.

Myneni, R.B., Ramakrishna, R., Nemani, R., Running, S.W., 1997. Estimation of global leaf area index and absorbed PAR using radiative transfer models. IEEE Trans. Geosci. Remote Sens. 35 (6), 1380–1393.

Oindo, B.O., Skidmore, A.K., 2002. Interannual variability of NDVI and species richness in Kenya. Int. J. Remote Sens. 23 (2), 285–298.

Olivas, P.C., Oberbauer, S.F., Clark, D.B., Clark, D.A., Ryan, M.G., O'Brien, J.J., Ordoñez, H., 2013. Comparison of direct and indirect methods for assessing leaf area index across a tropical rain forest landscape. Agric. For. Meteorol. 177, 110–116.

Pisek, J., Chen, J.M., Kobayashi, H., Rautiainen, M., Schaepman, M.E., Karnieli, A., Sprinstin, M., Ryu, Y., Nikopensius, M., Raabe, K., 2016. Retrieval of seasonal dynamics of forest understory reflectance from semiarid to boreal forests using MODIS BRDF data. J. Geophys. Res. Biogeosci. 121 (3), 855–863.

Pivovaroff, A., Sharifi, R., Scoffoni, C., Sack, L., Rundel, P., 2014. Making the best of the worst of times: traits underlying combined shade and drought tolerance of Ruscus aculeatus and Ruscus microglossum (Asparagaceae). Funct. Plant Biol. 41 (1), 11–24.

Rautiainen, M., Mõttus, M., Heiskanen, J., Akujärvi, A., Majasalmi, T., Stenberg, P., 2011. Seasonal reflectance dynamics of common understory types in a northern European boreal forest. Remote Sens. Environ. 115 (12), 3020–3028.

Rentch, J.S., Fajvan, M.A., Hicks, R.R., 2003. Oak establishment and canopy accession strategies in five old-growth stands in the central hardwood forest region. For. Ecol. Manage. 184 (1-3), 285–297.

Rocchini, D., Chiarucci, A., Loiselle, S.A., 2004. Testing the spectral variation hypothesis by using satellite multispectral images. Acta Oecol. 26 (2), 117–120.

Rouse, J.W., Haas, R.H., Schell, J.A., Deering, D.W. (1973), Monitoring vegetation systems in the Great Plains with ERTS, Third ERTS Symposium, Vol. I.

Rueden, C.T., Schindelin, J., Hiner, M.C., DeZonia, B.E., Walter, A.E., Arena, E.T., Eliceiri, K.W., 2017. Image J2: ImageJ for the next generation of scientific image data. BMC Bioinf. 18 (1), 529.

Running, S.W., 1994. Testing FOREST-BGC ecosystem process simulations across a climatic gradient in Oregon. Ecol. Appl. 4 (2), 238–247.

Running, S.W., Gower, S.T., 1991. FOREST-BGC, a general model of forest ecosystem processes for regional applications. II. Dynamic carbon allocation and nitrogen budgets. Tree Physiol. 9 (1–2), 147–160.

Ryu, Y., Lee, G., Jeon, S., Song, Y., Kimm, H., 2014. Monitoring multi-layer canopy spring phenology of temperate deciduous and evergreen forests using low-cost spectral sensors. Remote Sens. Environ. 149, 227–238.

Schaepman-Strub, G., Schaepman, M.E., Painter, T.H., Dangel, S., Martonchik, J.V., 2006. Reflectance quantities in optical remote sensing—Definitions and case studies. Remote Sens. Environ. 103 (1), 27–42.

Schleppi, P., Thimonier, A., Walthert, L., 2011. Estimating leaf area index of mature temperate forests using regressions on site and vegetation data. For. Ecol. Manage. 261 (3), 601–610.

Schuur, E.A.G., 2003. Productivity and global climate revisited: the sensitivity of tropical forest growth to precipitation. Ecology 84 (5), 1165–1170.

R Core Team, 2017. R: A Language and Environment for Statistical Computing. R Found. Stat. Comput., Vienna, Austria.

Thimonier, A., Sedivy, I., Schleppi, P., 2010. Estimating leaf area index in different types of mature forest stands in Switzerland: a comparison of methods. Eur. J. Forest Res. 129 (4), 543–562.

Weiss, M., Baret, F., Smith, G.J., Jonckheere, I., Coppin, P., 2004. Review of methods for in situ leaf area index (LAI) determination: Part II. Estimation of LAI, errors and sampling. Agric. For. Meteorol. 121 (1-2), 37–53.

Wright, I.J., Reich, P.B., Westoby, M., Ackerly, D.D., Baruch, Z., Bongers, F., Villar, R., 2004. The worldwide leaf economics spectrum. Nature 428 (6985), 821–827.

Yang, W., Kobayashi, H., Suzuki, R., Nasahara, K.N., 2014. A simple method for retrieving understory NDVI in sparse needleleaf forests in Alaska using MODIS BRDF data. Remote Sens. 6 (12), 11936–11955.

Yang, W., Kobayashi, H., Nasahara, K.N. (2015). Satellite Estimation of Overstory and Understory Leaf Area Index (LAIo & LAIu) in Boreal Forests. American Geophysical Union, Fall Meeting 2015, San Francisco, USA, 2015.

Zheng, G., Moskal, L.M., 2009. Retrieving leaf area index (LAI) using remote sensing: theories, methods and sensors. Sensors 9 (4), 2719–2745.

Zhu, G., Ju, W., Chen, J.M., Zhou, Y., Li, X., Xu, X., 2010. Comparison of forest Leaf Area Index retrieval based on simple ratio and reduced simple ratio. In: 2010 18th International Conference on Geoinformatics. IEEE, pp. 1–4.